

PROPERTIES OF HEAVY ION LINACS WITH ALTERNATING PHASE FOCUSING

H. Deitinghoff, P. Junior and H. Klein
 Institut für Angewandte Physik

Universität Frankfurt/Main, D6000 Frankfurt/M., FRG

Summary

General aspects for the application of alternating phase focusing are discussed. The results demand necessary linac parameters. The possibility of their accomplishment by already existing or feasible linac structures with acceleration rates of 2 - 3 MV/m will be considered.

For a heavy ion postaccelerator in the energy range from 1 to 6 MeV/N for Br ions typical properties of alternating phase focusing like choice of phase and frequency, phasedamping, energy-spread, and resulting consequences are specified. Computed radial and axial acceptances are given. For C^{6+} ions normalized radial acceptances (common area) of 2 cm mrad are achieved, for Br^{26+} the common area is still 0.8 cm mrad, both corresponding to axial bunches of $|\Delta\phi| = 5^\circ$ in phase and $|\Delta T/T| = 1\%$ in energy spread at the accelerator input. For this example a frequency of 108 MHz and an accelerating field strength of 2.5 MV/m are chosen. Finally sensitiveness on perturbations and shortage of linac sections are also taken into account.

Introduction

Conventional linacs in operation have accelerating fields of about 1 - 2 MV/m and correspond to the principle of a surf-rider. When synchronous particles are accelerated at a fixed phase with respect to the rf field, stable axial as well as radial motion can only be achieved by additional installation of alternating gradient focusing quadrupole lenses.

In a superconducting linac and some normal conducting new structures, where much higher acceleration rates (2 - 4 MV/m) become available, one can abandon the surf-rider principle and replace a. g. focusing by alternating phase focusing (APF).

This method was proposed by Good¹, Mullet² and Fainberg³ in the early fifties indeed, but an application appeared impossible then, since rf technics as well as necessary electric field strengths did not suffice. With the development of new structures such as the $\lambda/2$ -helix resonator, the reentrant cavity, spiral and splitting resonators APF became quite hopeful again, a fact which is emphasized by a series of new publications⁴⁻¹⁰.

Those resonators have some relevant advantages: higher rf fields, modular composition of linac, and consequently possibility of individual tuning rf phases and amplitudes in each cavity. In our institute a systematic theoretical research of APF

was done quite recently¹¹; some results concerning a linac for not too heavy ions are demonstrated in this paper.

Optical model

First we want to explain the basic principle of this method by help of an optical model of the linac. Particle motion is generally described by well-known equations of motion

$$\begin{aligned} \text{axially } \ddot{z} &= I_0(\gamma r) \frac{qe}{m} E_0 \cos[\omega t - \int k(z') dz' - \phi_s - \Delta\phi] \\ \text{radially } \ddot{r} &= -\frac{k}{\gamma} I_1(\gamma r) \frac{qe}{m} E_0 \sin[\quad] \end{aligned} \quad (1)$$

where r and z are cylindrical coordinates in laboratory frame, I_0, I_1 modified Bessel functions, q specific charge of ion, E_0 field amplitude, k wave number, γ radial wave number, ω angular frequency, ϕ_s synchronous phase. This system of coupled equations forms the base of our computational work, which will be shown later. For small radial ($\gamma r \ll 2$) and axial deviations ($\Delta\phi = ku \ll \phi_s$) equations transform to

$$\begin{aligned} \ddot{u} &= -\frac{qe}{m} E_0 k \sin\phi_s \\ \ddot{r} &= \frac{1}{2} \frac{qe}{m} E_0 k r \sin(\phi_s + \Delta\phi) \end{aligned} \quad (2)$$

where u is the axial coordinate, which moves along with the "synchronous" particle

$$u = z - vt.$$

"Synchronous" should be understood such that the field pattern is broken down by a Fourier analysis, where the fundamental wave component travels with increasing velocity along the direction of particles. Synchronous phase and phase deviations always refer to this wave¹². If we solve (2) by help of the "thin lens approximation" we get lens strengths or inversal focal lengths of our resonators

$$\begin{aligned} \frac{1}{f_{\text{axial}}} &= + \frac{qe}{m} \frac{\omega E_0}{v^3} l \sin\phi_s \\ \frac{1}{f_{\text{radial}}} &= - \frac{1}{2} \frac{1}{f_{\text{axial}}} \end{aligned} \quad (3)$$

A helix or spiral resonator with a length l (see Fig. 1) acts as a thin converging or diverging lens depending on the sign of the synchronous phase ϕ_s .

Now the idea of APF is based upon the possibility of phasing each resonator individually, such as they all may be tuned alternatively as converging and diverging lenses. As a consequence we come to a scheme (Fig. 2). This well-known "thin lens

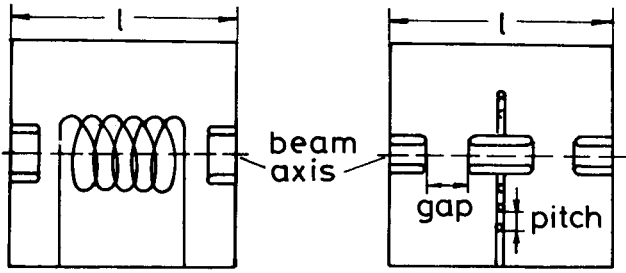


Fig. 1 Scheme of helix and spiral resonator

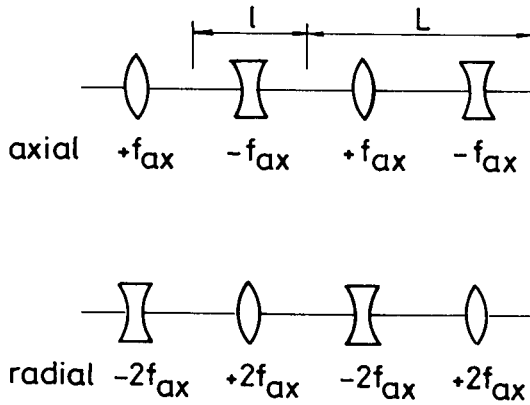


Fig. 2 Lens model of APF

scheme" proves quite useful for a discussion of questions such as:

1. What focal lengths of such periodic lens sequences submit stable axial (simple focal length) as well as radial (double focal length) motions?

2. Do realistic resonator parameters give satisfying acceptances?

The first question is answered by Floquet's theorem^{1,3}, which can very simply be derived by use of matrix theory of particle motion. Now the characteristic exponent μ must be introduced, which in case of our lens sequence has a very simple expression

$$\cos \mu = 1 - \frac{1}{2} \frac{l^2}{f^2} \quad (4a)$$

The stability condition $-1 < \cos \mu < +1$ splits into two, which must be satisfied simultaneously in our case

$$\text{axial} - 1 < 1 - \frac{l^2}{2f_{\text{axial}}^2} < +1$$

$$\text{radial} - 1 < 1 - \frac{l^2}{8f_{\text{axial}}^2} < +1$$

In case of stability synchrotron theory^{1,3} additionally supplies a formula for the

elliptic acceptance of our lens sequence

$$A = \frac{\pi R^2 \sin \mu}{l(2 + 1/f)} \quad (4b)$$

(4a) and (4b) make evident, that stability of motions depends only on a lens parameter $1/f$, which results from (3) multiplied by resonator length l .

$$\frac{1}{f} = \frac{qe}{m} \frac{\omega E_0}{v^3} l^2 \sin \phi_s \quad (5)$$

The acceptance then additionally depends on aperture radius R and resonator length l .

Characteristic exponent together with resulting radial and axial acceptances as functions of the lens parameters are shown in Fig. 3 for several symmetric lens arrangements. Fig. 3 suggests the following facts:

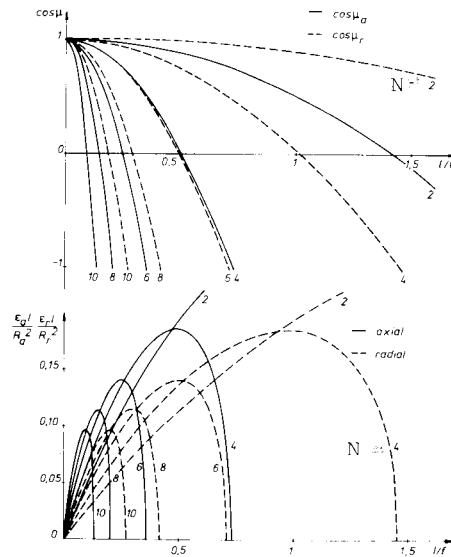


Fig. 3 Characteristic exponent and elliptical acceptance as functions of lens parameter $1/f$, $N = \text{lenses/period } L$.

1. Lens parameters should have an order of magnitude 1.

2. As a consequence of different radial and axial foci (3) maximum axial and radial acceptances cannot be gained simultaneously.

3. With more lenses per period maximum acceptances shift towards smaller lens parameters and become slightly larger for a chosen lens parameter.

Lens parameter (5) is determined by three relevant linac parameters namely particle velocity v , frequency ν and acceleration rate $qE_0 \sin \phi_s$. To have orders of magnitude 1 for lens parameters proper APF needs small velocities and large accelera-

tion rates, i. e. low energy protons and light ions with high charge states.

Nevertheless if we compare Fig. 3 and Table I realistic parameters still turn out small. In Table I data of some existing and designed linacs are put together with resulting lens parameters. Protons seem suitable for APF, light ions eventually in postaccelerators (1 - 6 MeV/N), Uranium should be eliminated for a postaccelerator. Therefore our example of a postaccelerator restricts us to light ions.

TABLE I

| Linac | Ions | E_0 [MV/m] | RF [MHz] | TT average | $T_{initial}$ [MeV/N] | T_{final} [MeV/N] | $1/f_{initial}$ | $1/f_{final}$ |
|---|-----------------|-----------------|-------------|---------------|--------------------------|------------------------|-----------------|---------------|
| superconducting helices | P | 1 - 2 | 90 | 1 | 0.75 | 6 | 0.2 | 0.07 |
| postaccelerator with $\lambda/2$ -helices | Br_{79}^{26+} | 2.5 | 108 | 1 | 1.8 | 6 | 0.14 | 0.02 |
| postaccelerator with spiral resonators | Br_{79}^{26+} | 2.5 | 108 | 0.9 | 1.8 | 6 | 0.3 | 0.04 |
| | C_{12}^{6+} | 2.5 | 108 | 0.8 | 7 | 12 | 0.2 | 0.025 |
| low energy helix | U_{238}^{11+} | 1 | 27 | 1 | 0.1 | 1.4 | 0.05 | 0.015 |

Computational results

Our optimization work is carried through within this optical lens frame. However, resulting exact computations are based on the general equations (1), which are solved by means of the Runge-Kutta-method.

Besides it should be emphasized that in our computations accelerating field amplitudes E_0 do not increase with particle velocity in order to preserve lens periodicity, but remain constant throughout acceleration. As a consequence lens parameters and focusing become weaker along the linac. Moreover all sections used in linac are presumed identical. Accordingly fields should be corrected with corresponding transittime factors. Mean transittime factors are taken as 1.0 for helices¹⁴, for spirals 0.9 in case of Br_{79}^{26+} , 0.8 in case of C_{12}^{6+} ¹⁵. For phase acceptances "walls" are taken as $-2\phi_s$ and $+2\phi_s$, radial aperture radius is taken as 2 cm.

At first let us explain our choice of linac parameters and how we are systematically forced towards a certain structure and corresponding parameters.

For a postaccelerator normal and superconducting helices and spiral resonators are taken into account, helix data being taken from¹⁴, spiral data from^{15,16}. The choice of frequencies is 54 and 108 MHz, accelerating fields are 2.5 MV/m. For the acceleration of Br_{79}^{26+} from 1.77 to 6 MeV/N some alternatives are:

- 34 $\lambda/2$ -helix resonators (length 33.7 cm) at 54 MHz
- 44 $\lambda/2$ -helix resonators (length 26.5 cm) at 108 MHz
- 27 spiral resonators (length 24.7 cm) at 54 MHz

32 spiral resonators (length 20.7 cm) at 108 MHz

at a synchronous phase ϕ_s of 30° .

Evidently there is a considerable difference in resonator lengths between helices and spirals, as helix together with necessary rf shielding must be chosen longer compared to spirals due to transit time considerations. Fig. 1 already showed length proportions required. In our examples spiral resonators are tied together such that 4 resonators respectively form a block and between each block a certain distance for vacuum and beam monitoring devices is provided. In case of superconducting helices 8 $\lambda/2$ -helices are stacked in a cryostat. Fig. 4 shows a remarkable difference between axial acceptances of a spiral and a helix linac, a fact, which is easily understood by the larger length of the helix and corresponding smaller effective acceleration rate (frequency is 108 MHz, synchronous phase switches from -10° to $+10^\circ$ after four resonators respectively).

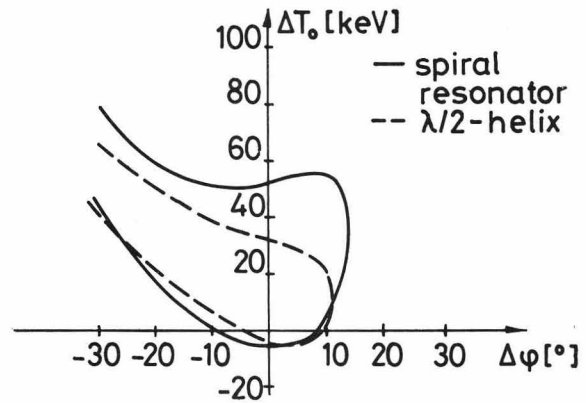


Fig. 4 Axial acceptances of helix and spiral postaccelerators (1.8 - 6 MeV/N, Br_{79}^{26+} , $\nu = 108$ MHz, $E_0 = 2.5$ MV/m, $\phi_s = \pm 10^\circ$)

Fig. 5 compares acceptances of a 54 MHz - to a 108 MHz - linac and distinctly demonstrates a certain superiority of the spiral at 54 MHz, as far as axial acceptances are concerned. But still the 54 MHz helix is comparable, radial acceptances not differing. Now for reasons of mechanical stability 54 MHz is no appropriate frequency for a spiral, the spiral conductor getting too long. The 54 MHz helix though with smaller stability failures must be eliminated too for adjustment reasons¹⁷. Therefore our further discussion deals with a 108 MHz spiral resonator linac alone.

With a 4 resonator bloc design mentioned above, we still have a choice of phase sequences $+-+-+-$ or $++--++--$ or $++++--$ without changing the linac structure.

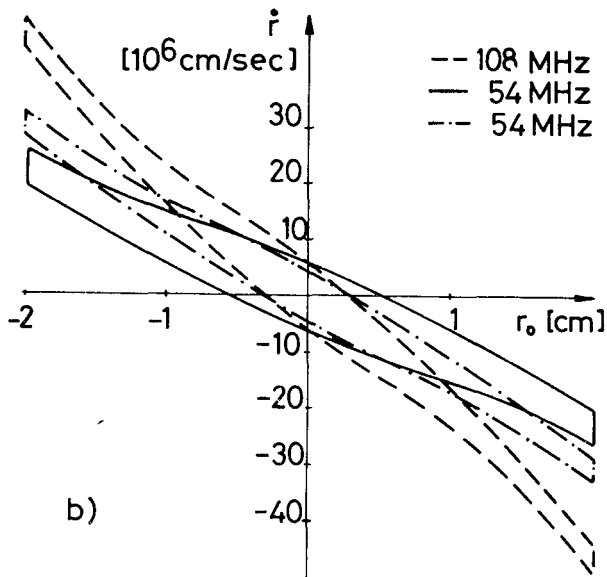
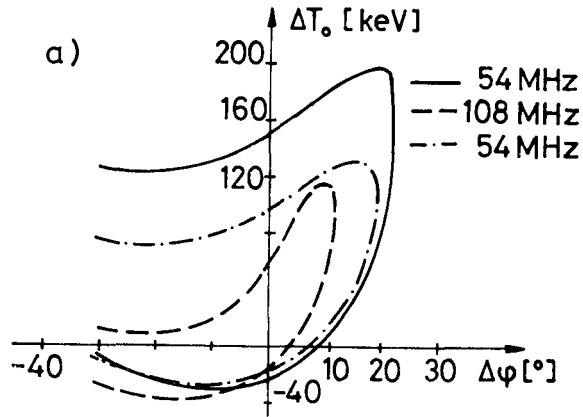


Fig. 5 Axial (a) and radial (b) acceptances of 54 MHz spiral linac (—), 108 MHz spiral linac (---), 54 MHz helix linac (- · -). (linac data s. Fig. 4; $\phi_s = \pm 30^\circ$)

Corresponding computational results in Fig. 6 indicate, that axial acceptances remain nearly constant while radial acceptances increase (in linear approximation this was already shown in Fig. 3 for small lens parameters).

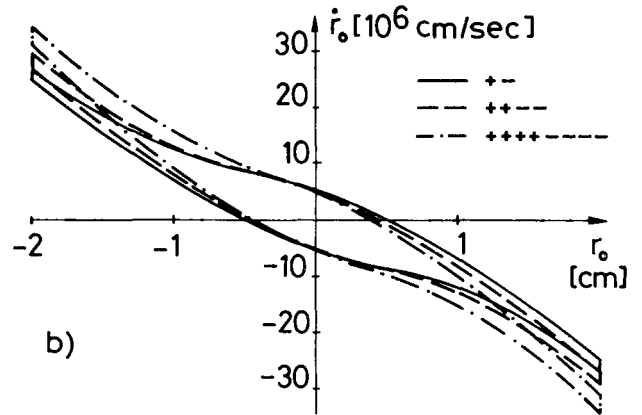
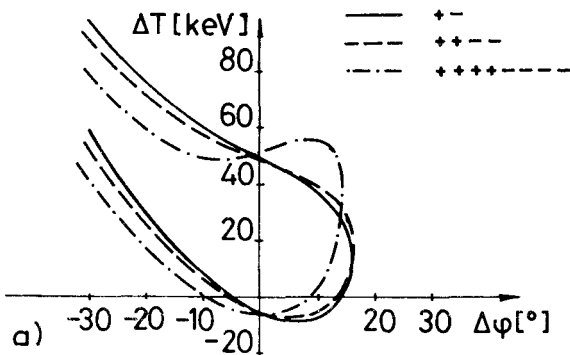


Fig. 6 Axial (a) and radial (b) acceptances with different lens sequences (data as in Fig. 4)

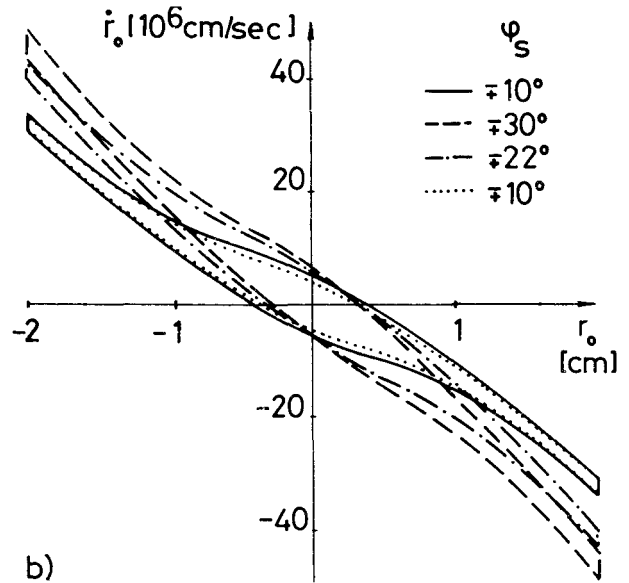
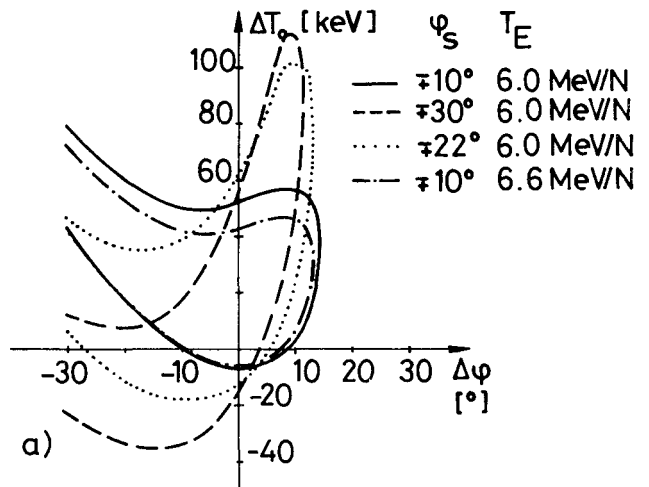


Fig. 7 Axial (a) and radial (b) acceptances as functions of synchronous phase (data as in Fig. 4)

A further interesting possibility is the choice of the synchronous phase itself. Fig. 7 demonstrates that at a given final energy radial as well as axial acceptances remain nearly unchanged, when a smaller synchronous phase angle is taken. This reduces investments, or if we hold on the number of sections for the sake of getting a higher energy, acceptances again decrease. Thus a relative weakness of this focusing method shows up since acceptances still depend on accelerator length.

Synchronous phase must not necessarily oscillate symmetrically⁵ between say $+10^\circ$ and -10° ; examples of nonsymmetric

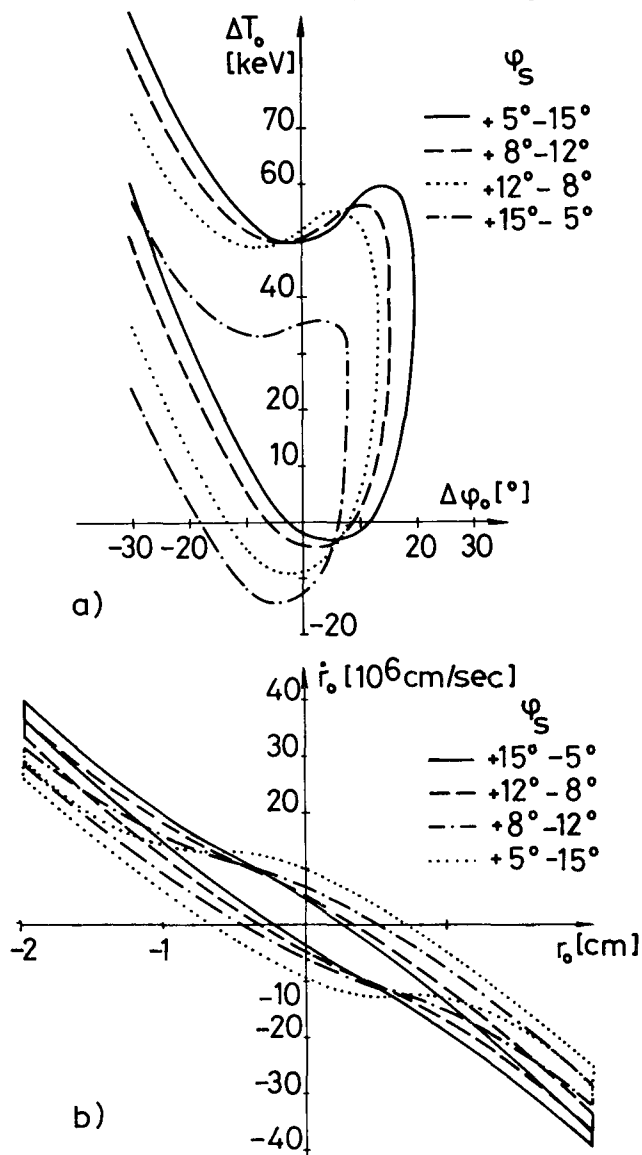


Fig. 8 Axial (a) and radial (b) acceptances as functions of nonsymmetric synchronous phase (data as in Fig. 4)

sequences are discussed in Fig. 8 giving opportunity of favouring one component of motion against the other. While axial acceptances remain quite untouched a distinct increase of radial acceptance is evident, thus focusing seems to improve by this step. But this improvement turns out small, when common sectional areas of radial acceptances for input particles with phase and energy deviations are considered.

As a summary of calculations axial and radial acceptances for the following ions C^{6+} , S^{15+} , Br^{23+} , and Br^{26+} are shown in Fig. 9 ($E = 2.5$ MV/m, $f = 108$ MHz, sequence $++++--$ of spiral resonators). With input data phase deviations $|\Delta \phi| = 5^\circ$ respectively 10° and energy spreads $|\Delta E|/E = 1\%$ resp. 2% common sectional areas of normalized radial acceptances are summarized in Table II. Calculations yield a small decrease of phase deviation and energy spread in the linac output.

Since tandem accelerators deliver emittances of about $0.2 - 0.4$ cm mrad APF may represent a possibility of focusing such a postaccelerator, provided the beam is properly matched axially as well as radially and adjustment errors of the linac are kept small.

We still have to look at the effects of disturbances in an alternating phase focused linac such as the influence of lower electric fields or even of shortage of sections.

While a linac focused by quadrupoles still guides the beam, even when a shortage of all sections happens, APF naturally is much more sensitive.

If we tolerate that acceptances decrease by say 10% a shortage of not more than 4 sections is permitted, provided shortage sections are not neighbours. To inaccuracies of phase adjustment, acceleration remains quite insensitive as Figs. 7 and 8 demonstrated. The influence of a lowered electric field strength E_0 indicates Fig. 10. Tolerance is about 20% but at the same time this figure makes clear how higher acceleration rates increase acceptances. Fig. 10 demonstrates effects of larger E_0 but these can be interpreted for increasing q as well, which is consistent with results of Fig. 9.

Considerations teach us that acceptances decrease, when certain final energies respectively final velocities are surpassed. This is easily understood by the decreasing lens parameter. Therefore at a given final energy, APF linacs should be built as short as possible.

TABLE II

| Ion | ϕ_s [$^\circ$] | $T_{initial}$ [MeV/N] | T_{final} [MeV/N] | $\Delta\phi_o$ [$^\circ$] | ΔT_o [keV/N] | βA [cmmrad] | $ \Delta\phi_o $ [$^\circ$] | $ \Delta T_o $ [$\%$] | βA^{**} [cmmrad] | $ \Delta\phi_o $ [$^\circ$] | $ \Delta T_o $ [$\%$] | βA^{**} [cmmrad] |
|---------------------------------|--------------------------|--------------------------|------------------------|--------------------------------|-------------------------|-----------------------|----------------------------------|----------------------------|----------------------------|----------------------------------|----------------------------|----------------------------|
| Br ₇₉ ²⁶⁺ | + 8 | -12 | 1.8 | 6 | 0 | 1.2 | 10 | 2 | 0.35 | 5 | 1 | 0.8 |
| S ₃₂ ¹⁵⁺ | +10 | -10 | 3 | 8.5 | 0 | 1.7 | 10 | 2 | 0.55 | 5 | 1 | 1.0 |
| C ₁₂ ⁶⁺ | +10 | -10 | 7 | 12.5 | 0 | 2.9 | 10 | 2 | 1.2 | 5 | 1 | 2.0 |

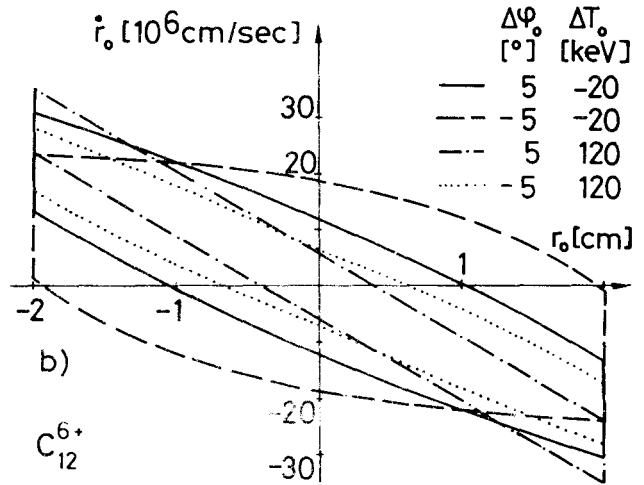
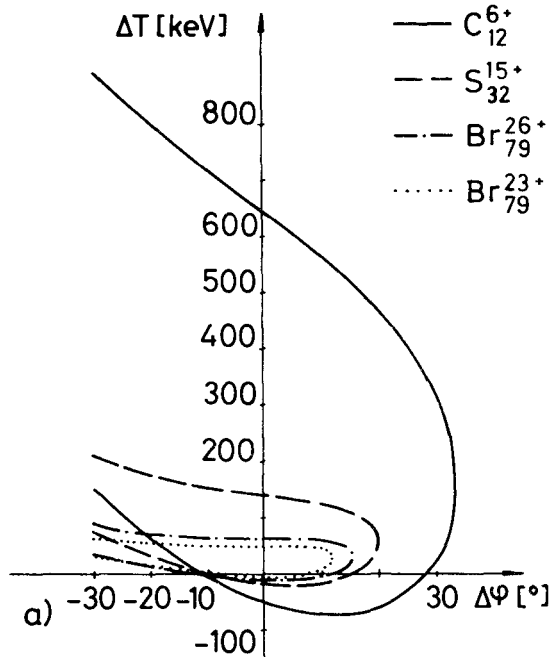


Fig 9a) Axial acceptances for different ions

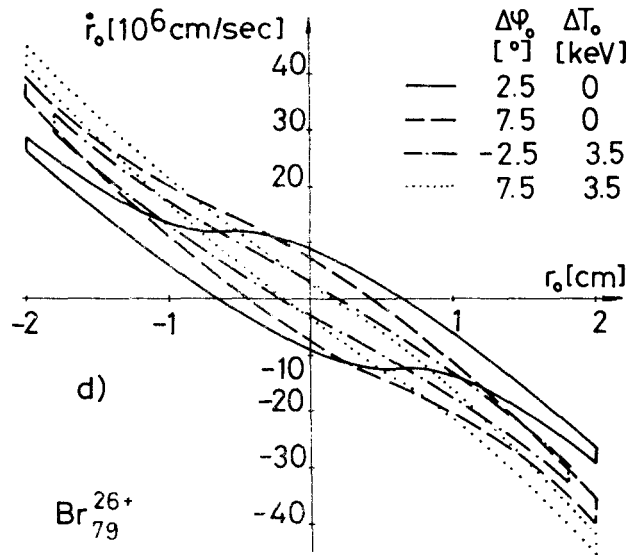
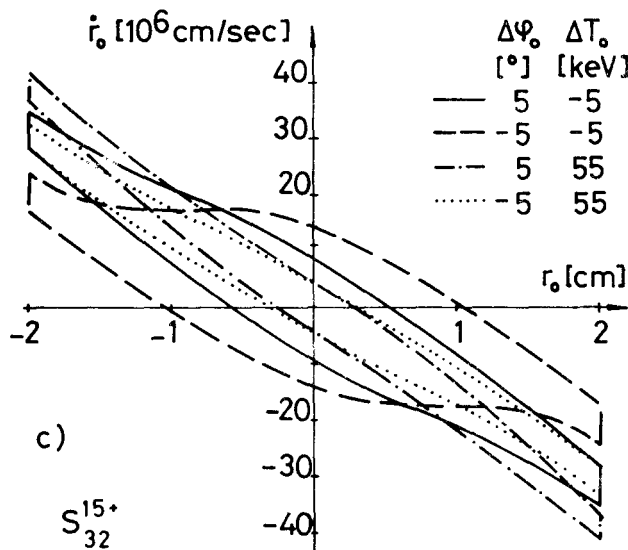


Fig 9 Common sectional areas for radial acceptances for

- b) C₁₂⁶⁺: $\phi_s = + 10^\circ, - 10^\circ$;
 $T_{in} = 7 \text{ MeV/N}; T_{fin} = 12.5 \text{ MeV/N}$
- c) S₃₂¹⁵⁺: $\phi_s = + 10^\circ, - 10^\circ$;
 $T_{in} = 3 \text{ MeV/N}; T_{fin} = 8.5 \text{ MeV/N}$
- d) Br₇₉²⁶⁺: $\phi_s = + 8^\circ, - 12^\circ$;
 $T_{in} = 1.8 \text{ MeV/N}; T_{fin} = 6 \text{ MeV/N}$

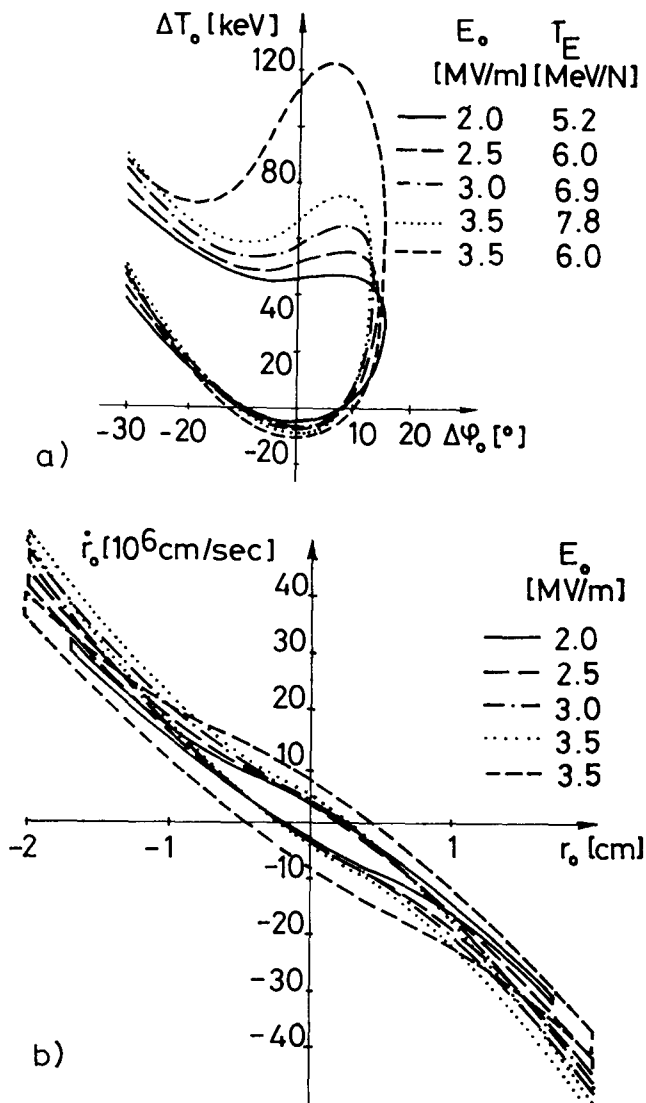


Fig. 10 Axial (a) and radial (b) acceptances as function of field strength (Initial energy 1.8 MeV/N, Br_{79}^{26+} , $\nu = 108$ MHz, $\phi = \pm 10^\circ$, variable final energy at constant section number and final energy 6.0 MeV/N at reduced section number)

Conclusions

The results indicate, that APF turns out as an alternative to conventional focusing for some applications. In this connection we present finally a comparison of an a. p. to a corresponding quadrupole focused spiral resonator linac. Normalized radial acceptances for synchronous particles turn out in case of Br_{79}^{26+} as

- 1.2 cm mrad for APF
- 3 cm mrad for N = 1 singlet focusing (3.6 - 5.4 kG/cm, R = 1.5 cm)
- 0.6 cm mrad for doublet focusing (2 - 3 kG/cm, R = 1.5 cm) with one doublet per 3 spirals

Singlets still admit a certain stock in acceptances necessary for a clean heavy ion machine, while at APF tolerances might become too small.

Acknowledgements

Work was supported by the Bundesministerium für Forschung und Technologie.

The computations were done at the Hochschulrechenzentrum, Universität Frankfurt/Main.

We thank Dr. A. Schempp for very informative discussions on the spiral resonator and Mrs. T. Harji for the careful drawings.

Literature

- 1 Good, M.L., Bull. Amer. Phys. Soc. 27, 6 (1952)
- 2 Mullet, L.B., AERE - GP/M - 147 (1953)
- 3 Fainberg, Y.B., CERN Symposium (1956)
- 4 Junior, P.H., Klabunde, J., Deitinghoff, H., Klein, H., Proc. 1970 Proton Lin. Acc. Conf., Batavia, Vol. 2, 759
- 5 Dreval', J. D., Kushin, V.V., Soviet Physics - Technical Physics Vol. 17, No. 9 (1973)
- 6 Chambers, E.E., HEPL No. 653, Stanford (1971)
- 7 Ben-Zvi, I., Ceperley, P.H., Schwettmann, H.A., HEPL No. 711, Stanford (1973)
- 8 Chambers, E.E., Ben-Zvi, I., HEPL No. 717, Stanford (1974)
- 9 Dreval', J.D., Kushin, V.V., Mokhov, V. M., Soviet Physics - Technical Physics Vol. 18, No. 9 (1974)
- 10 Swenson, D.A., LA-UR 15-1196 (1975) (Preprint)
- 11 Deitinghoff, H., Thesis Universität Frankfurt/Main (1975)
- 12 Livingstone, M.S., Blewett, J.P., Particle accelerators, McGraw Hill (1962)
- 13 Courant, E.D., Snyder, H.S., Annals of Physics 8, 1 (1958)
- 14 Deitinghoff, H., Klein, H., Kuntze, M., Vetter, J.E., Jaeschke, E., Repnow, R., KFK 2141 Karlsruhe (1975)
- 15 Schempp, A., Rohrbach, W., Klein, H., Nucl. Instr. Meth. (1976) in press
- 16 Schempp, A., Klein, H., this conference
- 17 as ¹⁴, page 22 ff.